

## Developmental kinetics, turnover, and stimulatory capacity of thymic epithelial cells

Daniel H. D. Gray, Natalie Seach, Tomoo Ueno, Morag K. Milton, Adrian Liston, Andrew M. Lew, Christopher C. Goodnow, and Richard L. Boyd

**Despite the importance of thymic stromal cells to T-cell development, relatively little is known about their biology. Here, we use single-cell analysis of stromal cells to analyze extensive changes in the number and composition of thymic stroma throughout life, revealing a surprisingly dynamic population. Phenotypic progression of thymic epithelial subsets was assessed at high resolution in young mice to provide a developmental framework. The cellular and molecular require-**

**ments of adult epithelium were studied, using various mutant mice to demonstrate new cross talk checkpoints dependent on RelB in the cortex and CD40 in the medulla. With the use of Ki67 and BrdU labeling, the turnover of thymic epithelium was found to be rapid, but then diminished on thymic involution. The various defects in stromal turnover and composition that accompanied involution were rapidly reversed following sex steroid ablation. Unexpectedly, mature**

**cortical and medullary epithelium showed a potent capacity to stimulate naive T cells, comparable to that of thymic dendritic cells. Overall, these studies show that the thymic stroma is a surprisingly dynamic population and may have a more direct role in negative selection than previously thought. (Blood. 2006;108:3777-3785)**

© 2006 by The American Society of Hematology

### Introduction

T-cell development in the thymus is essential for the establishment and maintenance of the adaptive immune system. Thymic stromal cells mediate various phases of thymocyte development to produce mature T cells capable of responding to foreign antigen while remaining tolerant of self. It is well established that different subsets of stromal cells form microenvironments in the thymic subcapsule, cortex, and medulla to facilitate distinct thymocyte maturational steps.<sup>1</sup> The maintenance of thymic microenvironments requires reciprocal interactions between thymocytes and stromal cells, termed thymic cross talk.<sup>2-4</sup> Although much is known about the biology of thymocytes, our understanding of thymic stromal cells is lacking.

The heterogeneity of murine thymic stromal cells has been demonstrated using monoclonal antibodies specific for various stromal determinants (eg, Godfrey et al<sup>5</sup>). These have proven useful in defining the epithelium, endothelium, fibroblasts, dendritic cells (DCs), and macrophages within thymic microenvironments. The cortex is characterized by a meshwork of reticular, cortical thymic epithelial cells (cTECs) that can be identified by distinctive patterns of intracellular (eg, MTS-44, K8) and surface (eg, Ly51) antigen expression.<sup>5-7</sup> Early T-cell development involves the migration of immature double-negative (DN, CD4<sup>-</sup>CD8<sup>-</sup>) thymocytes through the thymic cortex toward the subcapsule in close contact with cTECs.<sup>8</sup> At the subcapsule, lining fibroblasts facilitate DN thymocyte development through the provision of extracellular matrix components.<sup>9</sup> Maturing thymocytes then return through the cortex where cTECs mediate the process of positive selection,

rescuing T-cell receptor positive (TCR<sup>+</sup>) double-positive (DP; CD4<sup>+</sup>CD8<sup>+</sup>) thymocytes capable of interacting with self-peptide/MHC from programmed cell death.<sup>1</sup> Continued migration toward the medulla brings thymocytes in contact with DCs and medullary thymic epithelial cells (mTECs) that induce the apoptosis or anergy of potentially autoreactive thymocytes in a process termed negative selection.<sup>1,10,11</sup> Markers such as K5, MTS-10, and UEA-1 distinguish mTECs from cTECs, whereas differential expression of MHC II and B7 indicates further heterogeneity within the mTEC population.<sup>6,12,13</sup> Thymocytes surviving negative selection mature into CD4<sup>+</sup> or CD8<sup>+</sup> single-positive (SP) T cells within this microenvironment prior to export to the periphery.

Although immunohistologic analysis of TEC markers has revealed much about their development, there is a lack of quantitative data regarding their numerical relationship with thymocytes, turnover, capacity for regeneration, and function in thymocyte selection. Here, we use a refined method for isolating and analyzing thymic stromal cells at the single-cell level to address these issues. We found that stromal cell numbers changed markedly during thymic development and involution, maintaining a stable ratio with thymocytes after birth. This was associated with a surprisingly fast turnover and dynamic stage-specific phenotypic changes. These changes were dependent on thymocyte cross talk and RelB signals, including a newly defined role for CD40L in maintaining mTECs. TEC numerical and compositional defects that accompanied involution were promptly reversed on castration, demonstrating that the stroma retains the capacity to regenerate. In terms of TEC function

From the Monash Immunology and Stem Cell Laboratories (MISCL), Monash University, Victoria; the John Curtin School of Medical Research, The Australian National University, Canberra; The Australian Phenomics Facility, The Australian National University, Canberra; and the Walter and Eliza Hall Institute, Victoria, Australia.

Submitted February 17, 2006; accepted July 24, 2006. Prepublished online as *Blood* First Edition Paper, August 8, 2006; DOI 10.1182/blood-2006-02-004531.

An Inside *Blood* analysis of this article appears at the front of this issue.

The publication costs of this article were defrayed in part by page charge payment. Therefore, and solely to indicate this fact, this article is hereby marked "advertisement" in accordance with 18 USC section 1734.

© 2006 by The American Society of Hematology

in thymic selection, we test the abilities of distinct subsets as antigen-presenting cells (APCs), showing that subpopulations of mTECs and cTECs have surprisingly high capacity to stimulate naive T cells. This challenges the current view that TECs are poor APCs and suggests they may have a more direct role in negative selection than previously thought.

## Materials and methods

### Mice

C57BL-6 mice were maintained at the Alfred Medical Research and Education Precinct Animal Centre according to institutional guidelines. OT-I and gBT-I were gifts from Dr F. Carbone (Walter and Eliza Hall Institute, Victoria, Australia). RelB<sup>-/-</sup> mice were a gift from Dr W. Li (Walter and Eliza Hall Institute). CD40L<sup>-/-</sup> mice were housed at the Walter and Eliza Hall Institute. TCR $\alpha$ <sup>-/-</sup> and RAG-1<sup>-/-</sup> mice were housed at the John Curtin School for Medical Research.

### Castration

Anesthetized mice had a small scrotal incision made, and testes were tied-off with suture thread and removed with scissors. Sham-castrated mice received the incision, and the testes were exposed but not removed. Incisions were sealed with 9-mm autoclips (Becton Dickinson, Franklin Lakes, NJ).

### Antibodies

The following antibodies were used in this study: anti-CD31 (MTS-12), MTS-15,<sup>14</sup> MTS-10,<sup>15</sup> anti-Ly51 (6C3; Pharmingen, Palo Alto, CA), anti-EpCAM (G8.8a; gift from Dr A. Farr), anti-I-A/I-E (M5/114.15.2; Pharmingen), anti-H-2K<sup>b</sup> (AF6-88.5; Pharmingen), anti-CD40 (3/23; Pharmingen), anti-CD80 (IG10; gift from Dr D. Godfrey), anti-CD86 (GL1; Pharmingen), anti-CD45.2 (104; Pharmingen), anti-CD45 (30-F11; Pharmingen), anti-Ki67 (B56; Pharmingen), anti-BrdU (Pharmingen), rabbit anti-K5 (Covance, Berkeley, CA), anti-K8 (Troma-1; Developmental Studies Hybridoma Bank, Iowa City, IA). Secondary reagents were goat anti-rat IgG-FITC (Caltag, San Francisco, CA), rabbit anti-rat IgG-biotin (Vector, Burlingame, CA), and Streptavidin-CyChrome (Pharmingen).

### Thymic stromal cell isolation by enzymatic digestion

Thymic stromal cells were isolated as described previously.<sup>14</sup> Three adult or 10 embryonic thymi were pooled and digested in collagenase (Roche, Basel, Switzerland), then collagenase/dispase (Roche) and passed through 100- $\mu$ m mesh to remove debris.

### Flow cytometry

Immunofluorescent staining was performed as previously reported.<sup>14</sup> Sample data from  $1 \times 10^4$  CD45<sup>-</sup> cells were acquired on a FACScalibur (BD Biosciences, San Jose, CA) using up to 4 fluorescent channels and analyzed using CellQuest software (BD Biosciences). Where possible, propidium iodide was used to exclude dead cells.

### Thymic stromal cell purification

Stromal cells were incubated with anti-CD45 microbeads (Miltenyi Biotec, Bergisch Gladbach, Germany) in fluorescence-activated cell sorting (FACS) buffer. CD45<sup>+</sup> cells were depleted on an AutoMACS (Miltenyi Biotec) using the "Deplete\_S" program. CD45<sup>-</sup> cells were stained and sorted on a FACS Vantage (BD Biosciences) at fewer than  $3 \times 10^3$  cells/second to greater than 95% purity. Thymic and splenic dendritic cells were purified for polymerase chain reaction (PCR) by sorting CD11c<sup>hi</sup>/MHC II<sup>hi</sup> stromal cells. For proliferation assays, CD11c<sup>+</sup> cells were positively selected using AutoMACS beads to greater than 80% purity.

### Proliferation assays

Purified stromal cell subsets were incubated with OVA<sub>257-264</sub> or HSV gB<sub>498-505</sub> at 37°C for 60 minutes, and then washed thoroughly. Stromal cells (10 000) were plated with 50 000 splenic T cells purified using the pan-T-cell isolation kit (Miltenyi Biotec) from OT-I or gBT-I mice in U-bottom plates. Cells were cultured for 72 hours, in the presence of 1 mCi (37 MBq) <sup>3</sup>H-thymidine (Pierce, Rockford, IL) for the final 18 hours, and transferred onto filters on an Inotech cell harvester (Rockville, MA). Scintillant was added and filters were read on a beta-counter (Packard, Meriden, CT).

### Cytospins and immunohistology

Purified stromal cells were cytopun, fixed, and stained according to Jenkinson et al.<sup>16</sup> Immunohistology of mouse thymic cryosections was performed as described previously.<sup>14</sup> Images were acquired on a Bio-Rad MRC 1024 confocal microscope, equipped with a Nikon PlanApo 20 $\times$ /0.75 numerical aperture objective (Nikon, Tokyo, Japan), with a 3-line Kr/Ar laser using the acquisition software LaserSharp v 3.2 (Bio-Rad, Hercules, CA) and analyzed using LaserSharp processing software.

### Bromodeoxyuridine (BrdU) treatment and staining

Incorporation was initiated by intraperitoneal injection of BrdU (1 mg in PBS; Sigma, St Louis, MO) and maintained in drinking water (0.8 mg/mL BrdU). Thymic stromal cells were isolated and surface labeled, then fixed in 0.5% wt/vol paraformaldehyde (BDH Laboratory Supplies, Poole, United Kingdom), 0.01% Tween-20 (BDH Laboratory Supplies) in PBS overnight at 4°C. Cells were washed in PBS, recovered by centrifugation, and incubated in DNase I (50 Kunitz; Roche) for 30 minutes at 37°C. After washing, cells were stained with FITC-conjugated anti-BrdU (BD Biosciences) for 1 hour at room temperature.

### Ki67 staining

Cells were prepared and surface labeled as described previously. Samples were fixed and permeabilized using a Fix/Perm kit (BD Biosciences). After washing, cells were stained with FITC-conjugated anti-Ki67 for 30 minutes, then washed in preparation for flow cytometry.

### Reverse transcriptase PCR

Purified cells were resuspended in Trireagent (Molecular Research Center, Cincinnati, OH), and total RNA was recovered using BCP phase separation reagent (Molecular Research Center). Messenger RNA was reverse transcribed using Superscript II (Invitrogen, Carlsbad, CA) and oligo-dT (Invitrogen) incubated at 42°C for 90 minutes, followed by inactivation at 90°C for 5 minutes. PCR was performed using Taq polymerase (Promega, Madison, WI) and appropriate primers at annealing temperatures of 56°C (between 28 and 35 cycles for all tests; 35 cycles for HPRT).

### Quantitative PCR

Quantitative PCR was performed on a Corbett Rotor-Gene 3000 (Corbett Research, Sydney, Australia) using SYBRGreen supermix (Invitrogen) and 200 nM GAPDH or aire primers. Primer sequences were GAPDH, ACCATGTAGTTGAGGTCAATGAAGG, GGTGAAGGTCGGTGTG-AACG; aire, GGTTCTGTTGGACTCTGCCCTG, TGTGCCACGACG-GAGGTGAG.<sup>17</sup> After initial holds for 2 minutes at 50°C followed by 10 minutes at 95°C, the cDNA was amplified for 40 cycles at 95°C for 15 seconds, 60°C for 60 seconds. Three cDNA preparations of each stromal cell subset were analyzed, each in triplicate, and results were averaged after exclusion of outliers. Aire mRNA levels relative to those of GAPDH for the same cDNA preparation were determined with Corbett Rotor-Gene 6 software (Corbett Research) using the 2 Standard Curves Relative Quantitation method.<sup>18</sup> Relative aire mRNA expression levels in each thymic stromal cell subset were then calibrated to levels in whole CD45<sup>-</sup> thymic stromal cells (TSCs).

## Results

### CD45<sup>-</sup> thymic stromal cell numbers change with age

Given the lack of quantitative data regarding the thymic stroma, we first analyzed the numbers of CD45<sup>-</sup> stromal cells present during thymic ontogeny and involution. Total thymic cellularity (CD45<sup>+</sup> and CD45<sup>-</sup> cells) roughly doubled each day during fetal stages and continued to expand following birth until reaching a peak at 4 weeks of age (Figure 1A). Following puberty, thymic cellularity gradually decreased to neonatal levels by 12 months. CD45<sup>-</sup> cell numbers followed a similar trend, expanding rapidly during fetal and neonatal periods, until reaching an average peak of  $4.6 \times 10^5$  in 4-week-old mice (Figure 1B). On thymic involution CD45<sup>-</sup> cell numbers fell to an average of  $2.0 \times 10^5$  at 12 months.

As a proportion, CD45<sup>-</sup> thymic stromal cells composed 16% of the E14 thymus, representing an average thymocyte-to-stromal cell ratio of 5.5 (Figure 1B). On expansion of thymocytes, the stromal percentage was diluted to 1% by E18 and 0.5% of thymic cellularity following birth. Relatively small postnatal fluctuations in stromal cell proportion were more apparent in alterations of thymocyte-to-stromal cell ratios, which fell following puberty from an average of 440 to 280 (Figure 1C).

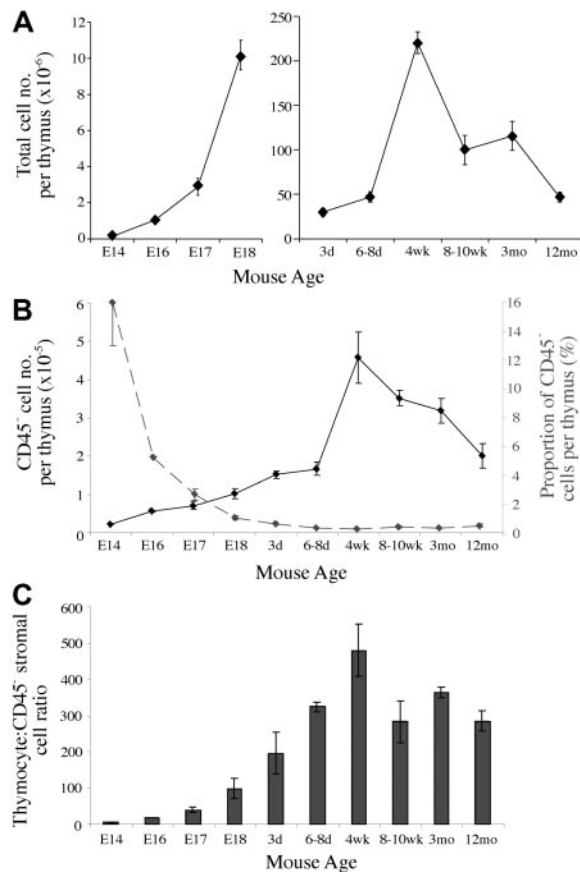


**Figure 1. Thymic stromal cells change in number and proportion throughout development.** (A) Graph of the total thymic cellularity at various ages. (B) CD45<sup>-</sup> thymic stromal cell number per thymus (solid line) and the proportion of thymic cellularity they compose (dashed line) at different ages. (C) Thymocyte-to-CD45<sup>-</sup> thymic stromal cell ratios at various time points. Means and standard errors from 2 to 5 experiments derived from digests of at least 3 thymi pooled for each time point are shown for all graphs.

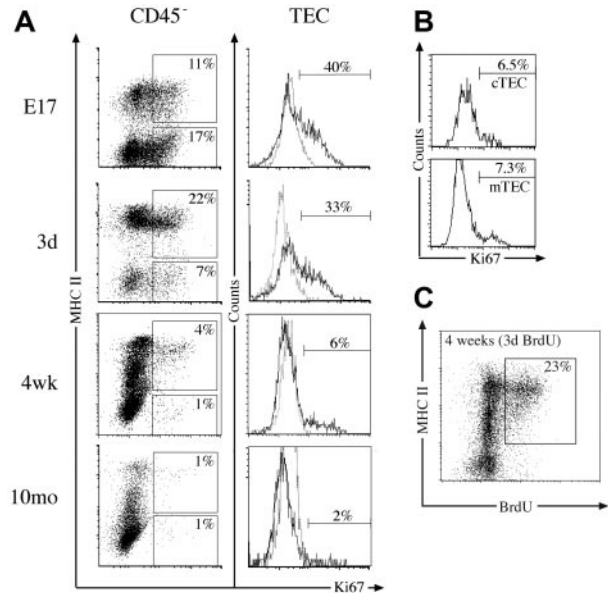


**Figure 2. Proliferation capacity of thymic stromal cells.** (A) Dot plots of MHC II versus Ki67 expression on CD45<sup>-</sup> thymic stromal cells at various time points, with regions indicating the proportion of Ki67<sup>+</sup> TECs (CD45<sup>-</sup>/MHC II<sup>+</sup>) and Ki67<sup>+</sup> non-TECs (CD45<sup>-</sup>/MHC II<sup>-</sup>). Histograms show Ki67 (solid line) and isotype control (dashed line) staining gated on TECs with markers indicating the proportion of Ki67<sup>+</sup> TECs. (B) Histograms of Ki67 expression on cTECs (CD45<sup>-</sup>/MHC II<sup>+</sup>/Ly51<sup>+</sup>) and mTECs (CD45<sup>-</sup>/MHC II<sup>+</sup>/Ly51<sup>-</sup>) from 4-week-old mice, with markers set according to isotype controls. (C) MHC II expression versus BrdU incorporated into 4-week-old CD45<sup>-</sup> stromal cells following 3 days of constant exposure. The proportion of CD45<sup>-</sup> cells that are BrdU<sup>+</sup> TECs is indicated. All plots are representative of 3 experiments performed.

Taken together, the marked expansion and contraction of stromal cell numbers and their relatively stable proportion following birth indicate dynamic population kinetics.

### Turnover of thymic epithelial cells

The extensive changes in thymic stromal cell numbers over time prompted examination of their proliferative status. Previous studies had quantified fetal TEC turnover *in vitro*<sup>19</sup> and adult turnover *in vivo*<sup>20</sup> by measuring BrdU incorporation. We first analyzed the thymic stroma directly for Ki67 expression as a marker of cell division<sup>21</sup> during phases of thymic growth, steady-state, and involution. Almost 30% of CD45<sup>-</sup> stromal cells were dividing at E17 and day 3 in both TEC and non-TEC compartments (Figure 2A). This fell to 5% of CD45<sup>-</sup> stromal cells at 4 weeks, most of which were TECs. By 10 months, both the number and proportion of Ki67<sup>+</sup> stromal cells had further diminished (Figure 2A; data not shown). This trend was reflected within the TEC subset, where extensive cell division was observed at E17 and in neonates (Figure 2A). Similar levels of Ki67 expression were observed within the cTEC and mTEC subsets at these time points (data not shown). Likewise, although the proportion of Ki67<sup>+</sup> TECs had fallen by 4 weeks, some cTECs and mTECs were dividing (Figure 2B). TECs expressing high levels of MHC II (MHC II<sup>hi</sup>) in 4-week-old and 12-month-old mice showed the most division (Figure 2A).

This was supported by analysis of BrdU incorporation during a 3-day continuous pulse in 4-week-old mice, where predominantly MHC II<sup>hi</sup> TECs retained the label (Figure 2C; data not shown). Within total CD45<sup>-</sup> stroma, 23% had proliferated in the previous 3 days, whereas 35% were BrdU<sup>+</sup> within the TEC subset (Figure 2C; data not shown). This indicates about 10% of

TECs arose from proliferation each day, and, given the relatively stable numbers of TECs between 4 and 12 weeks, this would translate to turnover of TECs every 10 to 14 days. Most of this proliferation, however, was restricted to the MHC II<sup>hi</sup> subset of TECs, perhaps suggesting these are transit-amplifying cells. Overall, these results show that stroma, in particular TECs, proliferate extensively during periods of thymic growth but divide less with thymic involution.

**Age-related alterations in stromal composition and TEC phenotype**

The marked changes in stromal cell number and turnover and the distinct roles stromal cell subsets have in thymocyte development prompted analysis of the composition of CD45<sup>-</sup> stroma in various thymic states. Although proportions of the major subsets were relatively stable throughout late ontogeny and young adulthood, marked differences were apparent in the middle-aged thymus. The proportion of TECs fell to less than half that of 4-week-old mice, whereas the percentage of fibroblasts and other non-TECs increased (Figure 3A-B). This was reflected by the ratio of TEC to fibroblasts, which was significantly lower in middle-aged compared with 4-week-old mice, possibly contributing to reduced thymic function (Figure 3D).

The composition of TECs was defined by analyzing expression of MHC II and the cTEC marker Ly51. Consistent with their role as APCs for developing thymocytes, all EpCAM<sup>+</sup> TECs expressed MHC II molecules. After 2 weeks of age, a significant population

of MHC II<sup>lo</sup> TECs emerged and expanded, becoming the predominant subset in the middle-aged thymus (Figure 3A,F). Using Ly51 expression to distinguish MHC II<sup>+</sup> cTECs and mTECs,<sup>14</sup> it was found that the E18 thymus harbored mainly cTECs expressing high levels of MHC II (Figure 3C). MHC II<sup>hi</sup> mTECs were increased in the neonatal thymus, giving a similar frequency of mTECs and cTECs (Figure 3C). This trend continued until 4 weeks, total mTECs outnumbered cTECs approximately 5-fold (Figure 3C,E). On thymic involution, mTEC number and proportion declined such that in 12-month-old mice, the mTEC/cTEC ratio had fallen from an average of 5.5 to 2.9 (Figure 3E).

The emergence of a significant population of MHC II<sup>lo</sup> TECs postnatally allowed discrimination of 4 major TEC subsets: MHC II<sup>hi</sup>/Ly51<sup>+</sup> (cTEC<sup>hi</sup>), MHC II<sup>lo</sup>/Ly51<sup>+</sup> (cTEC<sup>lo</sup>), MHC II<sup>hi</sup>/Ly51<sup>-</sup> (mTEC<sup>hi</sup>), and MHC II<sup>lo</sup>/Ly51<sup>-</sup> (mTEC<sup>lo</sup>). Although this is the first description of heterogeneity in cTECs defined by MHC II levels, the mTEC<sup>hi</sup> and mTEC<sup>lo</sup> populations are likely to correspond to those identified in previous histologic studies.<sup>22</sup> To determine the spatial localization and developmental relations of the subsets identified here, cTECs, mTEC<sup>hi</sup> subset, and mTEC<sup>lo</sup> subset were FACS purified, cytopun, and stained with antibodies to the keratin subunits K5 and K8. Previous studies suggested that K5<sup>+</sup>K8<sup>+</sup> TECs at the corticomedullary junction give rise to K5<sup>-</sup>K8<sup>+</sup> cTECs and K5<sup>+</sup>K8<sup>-</sup> or K5<sup>-</sup>K8<sup>+</sup> mTECs.<sup>6</sup> We found that indeed, the Ly51<sup>+</sup> cTEC population contained a major subset of K5<sup>-</sup>K8<sup>+</sup> cells and a minor subset of K5<sup>+</sup>K8<sup>+</sup> TECs (Figure 3G-H). The K5<sup>-</sup>K8<sup>+</sup> “globular” population of mTECs composed about 30% of the

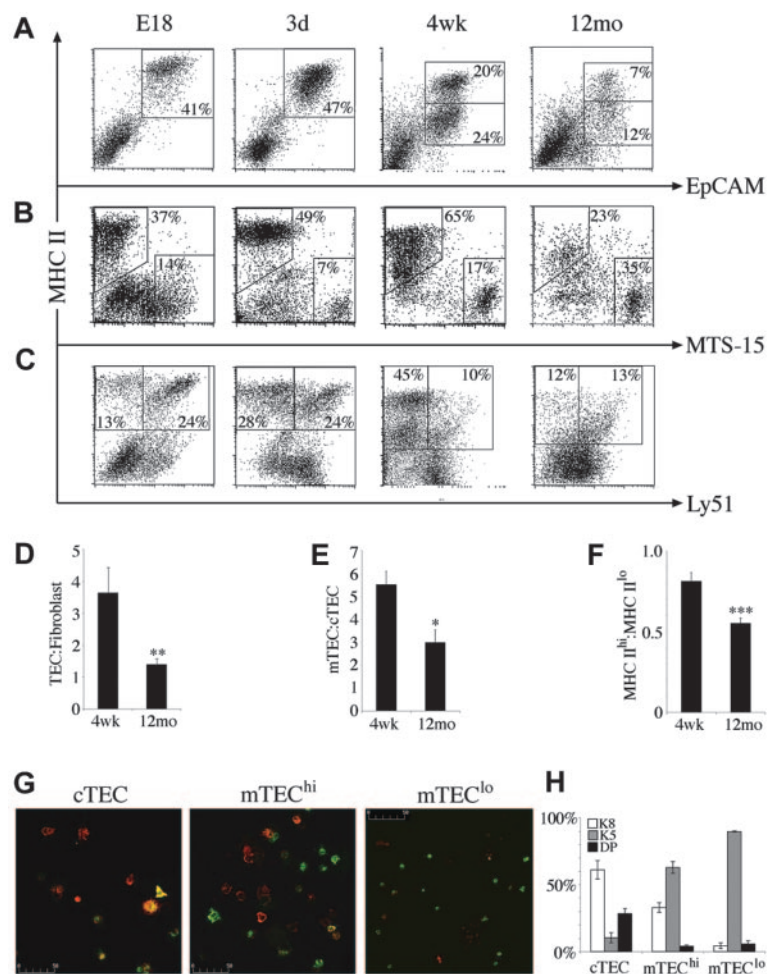
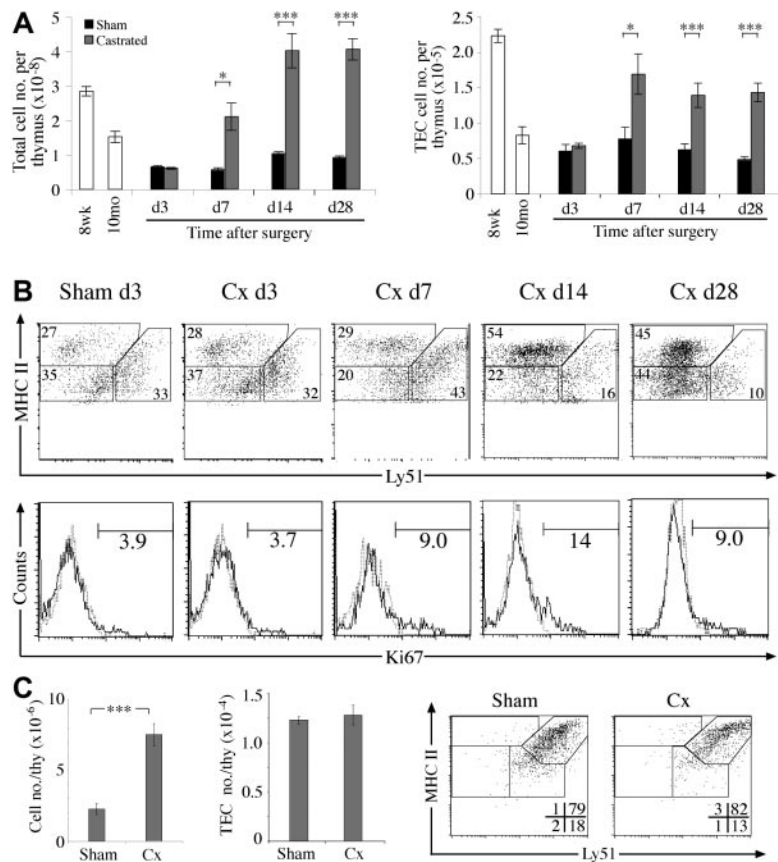


**Figure 3. Composition and phenotype of CD45<sup>-</sup> thymic stromal cells changes with age.** At various time points, CD45<sup>-</sup> stromal cells were stained for (A) MHC II versus EpCAM, (B) MHC II versus MTS-15, and (C) MHC II versus Ly51. Regions indicate CD45<sup>-</sup> stroma composed of TECs (MHC II<sup>hi</sup> and MHC II<sup>lo</sup> at adult time points), fibroblasts, cTECs (MHC II<sup>+</sup>/Ly51<sup>+</sup>), and mTECs (MHC II<sup>+</sup>/Ly51<sup>-</sup>). All dot plots are gated on CD45<sup>-</sup> thymic stromal cells isolated from at least 3 thymi pooled at the ages indicated and are representative of 2 to 5 experiments. Bar graphs of the ratios of (D) TEC/fibroblasts, (E) mTEC/cTEC, and (F) MHC II<sup>hi</sup>/MHC II<sup>lo</sup> TECs in 4-week-old and middle-aged (12-month-old) thymi. Means and standard errors are plotted, and groups were compared using a Mann-Whitney rank sum *U* test. (\**P* < .05, \*\**P* < .01, \*\*\**P* < .001). (G) Cytopins of purified cTECs, mTEC<sup>hi</sup> subset, and mTEC<sup>lo</sup> subset from 4- to 6-week-old mice stained with anti-K5 (green) and anti-K8 (red). (H) The mean proportion of TEC subsets that expressed K5, K8, or both (double positive, DP) with standard error from 3 experiments.

**Figure 4. Kinetics of TEC regeneration following surgical castration of aged mice.** (A) Total thymic cellularity and TEC number at various time points after castration or sham-castration of 10-month-old mice. (B) Dot plots of MHC II versus Ly51 expression on TECs (CD45<sup>-</sup>EpcAM<sup>+</sup>) from castrated or sham-castrated mice at various time points following surgery. Histograms show Ki67 expression on TECs with numbers showing the frequency of Ki67<sup>+</sup> TECs. All sham-castrated controls showed similar profiles and proportions to the day 3 control shown. (C) Total thymic and TEC number of castrated or sham-castrated 4-month-old RAG<sup>-/-</sup> mice 28 days after surgery. Means and standard errors are shown for all graphs from 5 mice per group, and a Student *t* test was used to determine statistical significance (\**P* < .05, \*\**P* < .01, \*\*\**P* < .001).



mTEC<sup>hi</sup> subset, whereas the remainder were K5<sup>+</sup>K8<sup>-</sup>, showing further phenotypic heterogeneity within this subset (Figure 3H). This was not the case for the mTEC<sup>lo</sup> population, which was almost uniformly K5<sup>+</sup>K8<sup>-</sup> (Figure 3G-H). Another interesting difference between mTEC<sup>hi</sup> and mTEC<sup>lo</sup> subsets was their size; mTEC<sup>lo</sup> cells were smaller than mTEC<sup>hi</sup> cells (data not shown; Figure 3G).

Together these data show the stroma undergo extensive compositional changes over time, particularly within the TEC fraction on thymic involution. This probably reflects changes in lymphostromal interactions and the reduced efficiency of thymic function.

#### Castration-induced regeneration of thymic stroma

To further test the ability of stromal cells to proliferate and remodel, we investigated whether the numerical and compositional defects of the involuted thymus could be corrected in a castration-induced model of thymic regeneration. As previously reported, total thymic cellularity of castrated middle-aged B6 mice rapidly increased compared with sham-castrated controls within 7 days, reaching normal young levels 14 days after surgery<sup>23</sup> (Figure 4A). We found that TECs also increased in number, showing that the atrophied stroma retains the capacity to regenerate. This numerical increase was accompanied by a return of mTEC/cTEC and MHC II<sup>hi</sup>/MHC II<sup>lo</sup> TEC ratios to normal young levels (data not shown). These compositional changes reflect a proportional increase of mTEC<sup>hi</sup> cells, most apparent 14 days following castration (Figure 4B). A similar increase in mTEC<sup>lo</sup> cells was observed by day 28, whereas the proportion of cTECs continued to fall. This TEC expansion appeared to derive at least in part from enhanced TEC proliferation, because the proportion of Ki67<sup>+</sup> TECs was higher than sham-castrated controls following day 7 (Figure 4B).

To determine the direct effects of sex steroid withdrawal on early thymocyte and stromal cell subsets, adult RAG-1<sup>-/-</sup> mice were castrated then analyzed 4 weeks later. The thymi of castrated RAG-1<sup>-/-</sup> mice expanded 3-fold compared with sham-castrated controls (Figure 4C). This was almost entirely due to increases of TN1-3 thymocytes (data not shown), as has been shown to occur in wild-type castrated mice.<sup>24</sup> Despite increased thymocyte numbers, castrate TEC numbers, phenotype, and proportions were no different to that of sham-castrates (Figure 4C). These data indicate that sex steroid withdrawal does not directly cause expansion of the early cTEC<sup>hi</sup> population or force their differentiation in the absence of mature thymocytes. In addition, the increased numbers of TN thymocytes was not sufficient to induce cTEC<sup>hi</sup> expansion.

#### Crosstalk requirements of adult TECs

The phenotypic progression of TECs apparent in early time points provided a basis to ascertain the signals that induce these subsets. The requirement for signals from developing thymocytes has previously been mapped to 2 distinct control points: (1) the presence of CD44<sup>-</sup>CD25<sup>+</sup> TN thymocytes to induce 3-dimensional arrangement of cTECs,<sup>25</sup> and (2) SP thymocyte induction or maintenance of mTECs.<sup>26</sup> However, the influence of these control points on the cTEC and mTEC subpopulations identified here and their quantitative relations with developing thymocytes are not known. To better define these requirements, TECs from RAG-1<sup>-/-</sup> (thymocyte development blocked at CD44<sup>-</sup>/CD25<sup>+</sup> TN) and TCR $\alpha$ <sup>-/-</sup> (blocked at DP) were analyzed (Figure 5A). RAG-1<sup>-/-</sup> epithelium was predominantly cTEC<sup>hi</sup> (Figure 5A), the main population observed in the fetal

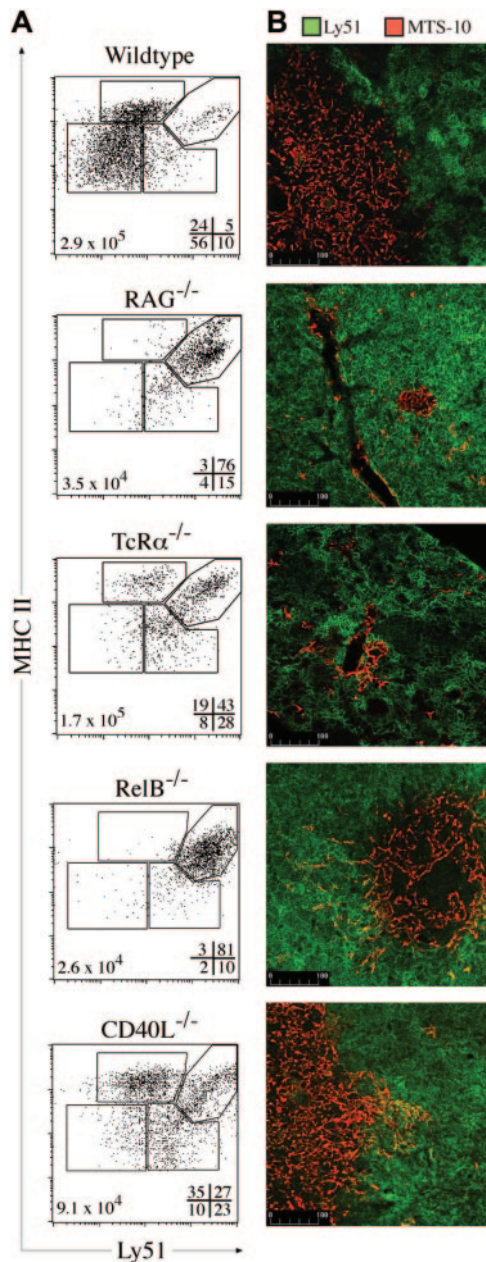


**Figure 5. Thymic cross talk requirements for TEC differentiation.** (A) MHC II and Ly51 expression on TECs (CD45<sup>+</sup>-EpCAM<sup>+</sup>) from wild-type, RAG-1<sup>-/-</sup>, TcRα<sup>-/-</sup>, RelB<sup>-/-</sup>, and CD40L<sup>-/-</sup> mice. Gates discriminate MHC II<sup>hi</sup> and MHC II<sup>lo</sup> cTEC and mTEC subpopulations, with the frequencies of each shown at the bottom right of each plot and total TEC numbers at the bottom left. Representative plots from 3 to 5 experiments are shown. (B) Ly51 (green) and MTS-10 (red) staining of thymic sections from wild-type and the various mutant mice. The MTS-10<sup>+</sup> areas in RAG-1 and RelB were infrequent compared with the other models examined. Representative images from 4 experiments are shown.

thymus and at lower proportions in the adult. The presence of DP in the TCRα<sup>-/-</sup> thymus maintained significant populations of cTEC<sup>lo</sup> and mTEC<sup>hi</sup> subsets, but not mTEC<sup>lo</sup> (Figure 5A), revealing a new checkpoint for adult TECs. Ki67 staining of mutant TEC subsets indicated they had similar proliferation to their wild-type counterparts (data not shown).

By immunohistochemistry, RAG-1<sup>-/-</sup> thymi exhibited bright, confluent Ly51 staining and some scattered MTS-10<sup>+</sup> cells (perhaps the few Ly51<sup>-</sup> TECs detected by FACS) (Figure 5B). In the TCRα<sup>-/-</sup>, DP and the increased numbers and proportion of cTEC<sup>lo</sup> subsets gave “stretched” and patchy Ly51 staining,

resembling the wild-type thymus (Figure 5B). Overall, these data show that DN and DP thymocytes induce the development or expansion of adult cTEC<sup>hi</sup> and cTEC<sup>lo</sup> subsets, respectively.

To define potential molecular mediators of cross talk-induced TEC differentiation and/or maintenance, we focused on the noncanonical NFκB signaling pathway that has been shown to be important for mTEC development.<sup>27</sup> RelB<sup>-/-</sup> mice are deficient in mTECs and DCs, although T-cell development is apparently normal.<sup>28</sup> RelB<sup>-/-</sup> TECs closely resembled those of RAG-1<sup>-/-</sup> mice in number and phenotype, arrested at the cTEC<sup>hi</sup> stage (Figure 5A). The few detectable mTECs formed rare, sparse medullary islets (Figure 5B). Although upstream elements that signal through the noncanonical NFκB pathway cause medullary defects<sup>27</sup> (eg, LTβR, TRAF-6, NIK), these are not as profound as the medullary block observed in RelB<sup>-/-</sup>. This suggests that several membrane receptors may transduce distinct signals, all requiring RelB, for aspects of mTEC (and perhaps cTEC<sup>lo</sup>) differentiation and/or proliferation.

One candidate, the TNF-receptor family member CD40, signals via the NIK-dependent NFκB pathway.<sup>29</sup> Mice deficient in CD40L exhibited numerical and proportional deficiency in the mTEC<sup>lo</sup> subset, despite exhibiting normal numbers of SP thymocytes (Figure 5A; data not shown). Although the TEC subset distribution resembled that of TCRα<sup>-/-</sup> mice, there were proportionally more mTEC<sup>hi</sup> present that presumably formed the large MTS-10<sup>+</sup> medullary areas (Figure 5A-B). This gave the appearance of a normal thymic microenvironment as previously reported for CD40L<sup>-/-</sup>.<sup>30</sup> Overall, these data identify a requirement for RelB at the early checkpoint of adult TEC progression and uncover a new role for CD40 in mTEC<sup>lo</sup> induction.

#### T-cell-stimulatory capacity of stromal cell subsets

We next investigated the functional capacity of TEC subsets. The processes of thymic positive and negative selection are primarily governed by thymocyte TCR interactions with stromal MHC/peptide complexes in a manner thought to be analogous to peripheral T-cell activation. Previous studies showed that thymic nurse cells (a cTEC subpopulation) stimulated T-cell hybridomas very poorly.<sup>31,32</sup> To determine whether poor APC function was a feature of all TEC subsets, we purified cTEC, mTEC<sup>hi</sup> subset, mTEC<sup>lo</sup> subset, and thymic DCs to assay their capacity to present cognate peptide to naive TCR transgenic cytotoxic T cells. In addition to postsort FACS analysis, quantitative PCR of TEC subsets for CD11c transcripts confirmed the absence of contaminating DCs (0.2%-0.3% of DC levels). Figure 6A shows that, as expected, thymic DCs elicited the greatest proliferative response from OT-I T cells. Surprisingly, cTECs and mTEC<sup>hi</sup> subset also induced high levels of naive T-cell proliferation, albeit lower than DCs. The mTEC<sup>lo</sup> subset delivered comparatively weak stimulation, showing that in this system their ability to present peptide and stimulate T cells was poor (Figure 6A). Similar trends were observed with HSV gB-specific CD8<sup>+</sup> T cells,<sup>33</sup> but with reduced differences among TEC subsets (Figure 6B).

To determine possible reasons for these differences we analyzed MHC and costimulatory molecule expression on purified stromal cells. The surface expression of H-2K<sup>b</sup> was similar among TECs and DCs, indicating the differences were not due to levels of peptide/MHC complexes (Figure 6D). PCR analysis of costimulatory molecule transcripts revealed that thymic DCs expressed higher levels than whole TECs (Figure 6C). Within TEC subsets, mTEC<sup>hi</sup> subset contained greater costimulatory molecule transcript levels than the mTEC<sup>lo</sup> subset, with cTEC levels falling between

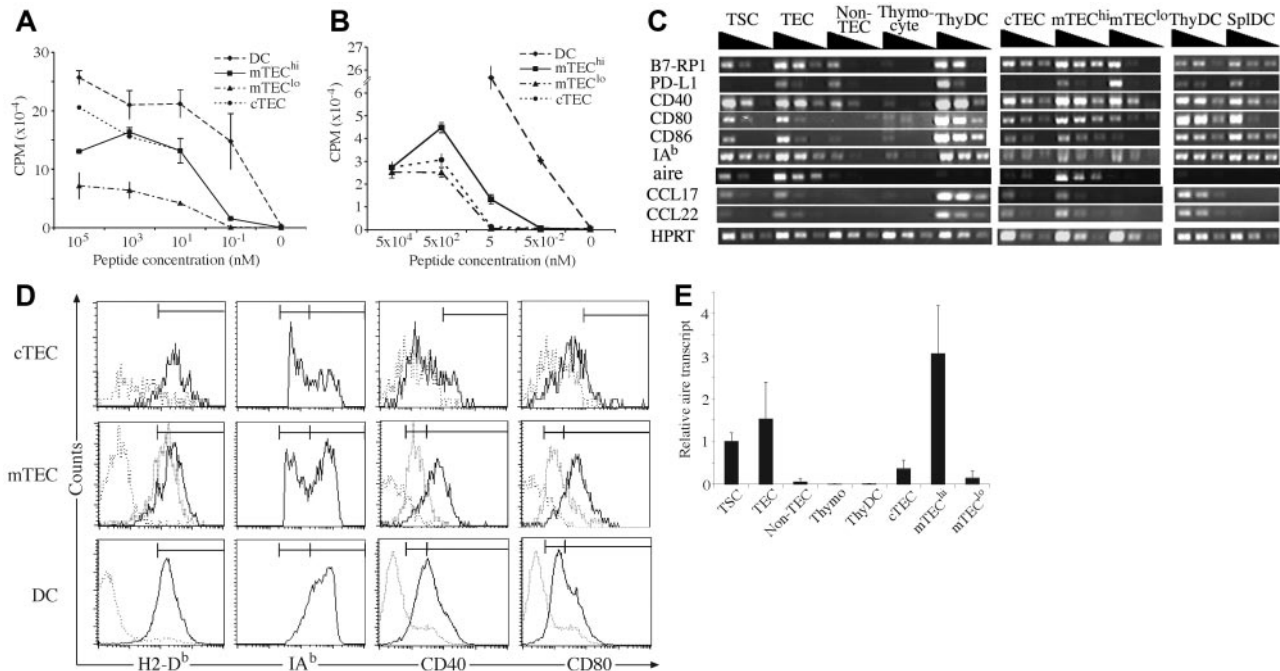


**Figure 6. Presentation and stimulation capacity of thymic stromal subsets.** Proliferative responses of naive OT-I (A) or gBT-I (B) TcR transgenic T cells stimulated by purified thymic stromal cells coated with various concentrations of cognate peptide. Limiting numbers of cTECs restricted their analysis to only certain peptide concentrations within each experiment; however, similar results were obtained throughout. (C) PCR analysis of costimulatory molecules, MHC II, aire, and chemokine transcripts in purified stromal cell subsets. (D) Histograms of H2-D<sup>b</sup>, IA<sup>b</sup>, CD40, and CD80 expression by thymic stromal subsets (solid line indicates cTECs, mTEC<sup>hi</sup> subset [except for IA<sup>b</sup> plot], and DCs; dashed line, mTEC<sup>lo</sup> (except for IA<sup>b</sup> plot); dotted lines, isotype controls). Markers are set to compare expression levels in positive populations. (E) Quantitative PCR analysis of aire transcript levels in purified thymic stromal cell subsets normalized for GAPDH expression. Means and SD generated from 3 different cDNA templates for each population are shown relative to whole TSCs.

these 2 (Figure 6C). This was supported by flow cytometric analysis of CD40, CD80, and CD86, with much higher surface levels found on mTEC<sup>hi</sup> compared with mTEC<sup>lo</sup> (Figure 6D; data not shown). Interestingly, thymic DCs exhibited surface levels of CD40 and CD80 that were between those of mTEC<sup>hi</sup> and mTEC<sup>lo</sup> populations. Small shifts in cTEC profiles indicated that only a subset of these cells express CD40, CD80, and CD86 (Figure 6D). We also analyzed the expression of other molecules important to thymic negative selection; autoimmune regulator (aire), which influences expression of tissue-specific antigens in the thymus,<sup>34</sup> and the chemokines CCL17 (TARC) and CCL22 (MDC) that have been proposed to attract DP thymocytes to the sites of negative selection.<sup>35</sup> Both endpoint and quantitative PCR showed transcript for aire almost exclusively in the mTEC<sup>hi</sup> subset (Figure 6C,E). In addition, the highest transcript levels of CCL17 and CCL22 were found in DCs and mTEC<sup>hi</sup> subsets (Figure 6C). Together, these data show that thymic DCs and mTEC<sup>hi</sup> subsets are “armed” with high levels of molecules important for negative selection, and that cTECs and mTEC<sup>hi</sup> subsets are surprisingly competent APCs.

## Discussion

It is well established that the heterogeneous thymic stroma is essential for T-cell development. Our knowledge of fundamental aspects of stromal cell biology, however, has been limited by a lack of quantitative and functional analysis. How many stromal cells are there in a normal thymus? Do they change in composition or phenotype throughout life? What are the stages of TEC development and turnover? How well are these cells equipped to induce central tolerance? In this study we sought answers to these

questions using single-cell analysis and purification of these technically problematic populations.

As a single population, CD45<sup>-</sup> stromal cells in abundance closely followed changes in overall thymic cellularity indicating a surprisingly dynamic behavior. The maintenance of a stable ratio with thymocytes after birth is likely to ensure appropriate cell-to-cell contact for important processes such as negative selection. Disruption of these ratios may lead to reduced interactions and autoimmunity, as has recently been proposed by Boehm et al.<sup>36</sup> A high level of proliferation supported these growth characteristics, with an estimated turnover time of 10 to 14 days for the 4-week-old TEC compartment; however, further kinetic studies will be required to confirm and compare TEC turnover.<sup>20</sup> Nevertheless, such growth characteristics would be slower than that reported for gut epithelium, faster than hepatocytes, and on par with skin epithelium.<sup>37</sup> In agreement with Yang et al.,<sup>38</sup> postnatal TEC division predominantly occurs in the mTEC<sup>hi</sup> population, contrary to the view that these represent postmitotic, end-stage cells. These data prompt a detailed analysis of TEC differentiation and how it relates to promiscuous gene expression.

The proportion of dividing non-TEC, then TECs diminished with age, reflecting or causing the stromal compositional changes that characterized the involuted thymus. Whether reduced TEC proliferation drives involution remains an open question; however, massive thymic hypertrophy in K5-cyclin-D1 transgenic mice indicates that TEC proliferation can control thymus size.<sup>39</sup> The numerical changes and phenotypic and proliferative defects of the involuted stroma were reversed by sex steroid ablation, showing that in middle-aged mice, the stroma retains the capacity to regenerate. This occurred with rapid kinetics and expansion of the

mTEC<sup>hi</sup> subset followed by the mTEC<sup>lo</sup> subset, perhaps recapitulating the stages of TEC development, resembling the sequential expansion of thymocyte subsets previously shown in this model.<sup>24</sup>

Surprisingly, the young and regenerated thymus contained a relatively low proportion of cTECs compared with mTECs. Three-dimensional reconstruction of thymus histology indicates that the cortex occupies 3 times more volume than does the medulla,<sup>40,41</sup> but the medulla is more densely packed with keratin, whereas cTECs appear “stretched.” Although we took care to assay TECs in all fractions of the digestion, we cannot exclude that specific loss of cTECs during isolation could occur. A recent study of mice expressing GFP only in TECs, however, showed a very low frequency of green cells in the cortex, compared with a high frequency in the medulla (H. R. Rodewald, personal written communication, September 12, 2005). This indicates that the adult cortex is established by relatively few cTECs extending long processes, whereas the medulla harbors greater numbers of more compact epithelial cells.

To better characterize the phenotypic and quantitative requirements for cross talk in the cortex and medulla, the stromal composition of various mutant mice was analyzed. In the TCR $\alpha^{-/-}$  thymus, DP or  $\gamma\delta$ TCR<sup>+</sup> SP thymocytes induced the RelB-dependent development or proliferation of cTEC<sup>lo</sup> and mTEC<sup>hi</sup> subsets. In light of previous studies, we consider it likely that DP induce expansion of cTEC<sup>lo</sup>, whereas  $\gamma\delta$ TCR<sup>+</sup> SP may give rise to the low proportion of the mTEC<sup>hi</sup> subsets observed.<sup>2</sup> Whether thymocytes affect the differentiation, proliferation, and/or maintenance of the adult cTEC<sup>lo</sup> and mTEC<sup>lo</sup> subsets requires further investigation. Regardless, these data map a new control point in cross talk that better resolves our understanding of TEC development. The differential regulation of cTEC<sup>hi</sup> and cTEC<sup>lo</sup> subsets by DN and DP may also imply these subsets have distinct functions in immature thymocyte development.

Collectively, cTECs had a surprisingly high capacity to stimulate the naive TCR transgenic T cells tested here. Although previous studies found thymic nurse cells (TNCs) were poor antigen-presenting cells,<sup>31,32</sup> this stromal subset comprises only a small subpopulation of cTECs. In contrast, the present study assayed all Ly51<sup>+</sup> TECs, which includes most, if not all, cTEC types (Figure 3H; D.H. D.G. and R.L.B., unpublished observations, September 2005). Furthermore, the predominance of TNCs in the outer cortex<sup>42,43</sup> suggests that the more stimulatory cTECs reside near the cortico-medullary junction. This has bearing on the ongoing argument over whether cTECs are capable of inducing negative selection<sup>44</sup> by demonstrating some of these cells express levels of MHC and costimulatory molecules that could delete thymocytes bearing TCR with high enough avidity for epithelial derived antigens.

Although previous experiments with TEC lines found that mTECs were competent APCs,<sup>45</sup> we extend these findings to show primary mTEC<sup>hi</sup> subsets are more likely to have a direct role in negative selection than mTEC<sup>lo</sup> subsets. In addition to the almost

exclusive expression of aire and the highest representation of peripheral transcripts<sup>46</sup> (mTEC<sup>hi</sup> correspond to CD80<sup>hi</sup> mTECs, Figure 6C), this subset has a potent capacity to stimulate peripheral T cells. This is likely to reflect a direct role for mTEC<sup>hi</sup> subsets in negative selection and is probably the subset responsible for TEC-mediated tolerance observed in other systems.<sup>13,47,48</sup> The implied hierarchy of stimulatory capacity among thymic stromal subsets (ie, DC, then mTEC<sup>hi</sup> and cTEC, then mTEC<sup>lo</sup>) correlated best with the expression of costimulatory molecules. These molecules have previously been shown to play important roles in deletion<sup>49-51</sup> and regulatory T-cell selection.<sup>52</sup>

The presence of some mTEC<sup>hi</sup> was not dependent on signals from  $\alpha\beta$ TCR SP thymocytes, as evidenced in fetal development and the TCR $\alpha^{-/-}$  thymus; however, they were required for their proportional expansion. The requirement for mature, CD40L<sup>+</sup> thymocytes is greater in the mTEC<sup>lo</sup> compartment. This is supported by the finding that CD40L overexpression on thymocytes causes massive expansion of mTECs at the expense of cTECs.<sup>30</sup> CD40 signaling is transduced via a NIK and RelB-dependent pathway, both of which are required for mTEC development or expansion. Whether this requires direct stimulation of mTEC<sup>lo</sup>, or acts via another stromal cell type (eg, DC, cTEC, mTEC<sup>hi</sup>) remains to be determined. Nevertheless, together these data establish CD40 as an important surface receptor in SP cross talk to a major subset of adult mTECs.

In conclusion, this study defines a very dynamic thymic stromal cell compartment, with rapid turnover of TECs and the capacity to regenerate following involution. The phenotypic progression of TECs and the fine mapping of their cellular and molecular cross talk requirements provides a framework to study epithelial differentiation. In addition, the ability of TECs to stimulate respectable proliferative responses from naive T cells suggests they may have a more direct role in negative selection than previously thought.

## Acknowledgments

We thank Drs D. Godfrey, A. Farr, L. Wu, and F. Carbone for their generous gifts of antibodies and mice and T. Heng, G. Goldberg, S. Sakkal, and J. Barbuto for mouse castrations.

This work was supported by grants from the Australian National Health and Medical Research Council (NH&MRC), Norwood Immunology, and the Australian Stem Cell Centre.

## Authorship

R.L.B. is Chief Scientific Officer of Norwood Immunology Ltd.

Correspondence: Richard Boyd, Monash Immunology and Stem Cell Laboratories (MISCL), Level 3, STRIP, Building 75, Monash University, Wellington Road, Clayton, Victoria, 3800, Australia; e-mail: richard.boyd@med.monash.edu.au.

## References

- Anderson G, Jenkinson EJ. Lymphostromal interactions in thymic development and function. *Nat Rev Immunol.* 2001;1:31-40.
- van Ewijk W, Shores EW, Singer A. Cross talk in the mouse thymus. *Immunology Today.* 1994;15:214-217.
- Gray DH, Ueno T, Chidgey AP, et al. Controlling the thymic microenvironment. *Curr Opin Immunol.* 2005;17:137-143.
- Jenkinson WE, Rossi SW, Jenkinson EJ, Anderson G. Development of functional thymic epithelial cells occurs independently of lymphostromal interactions. *Mech Dev.* 2005;122:1294-1299.
- Godfrey DI, Izon DJ, Wilson TJ, Tucek CL, Boyd RL. Thymic stromal elements defined by mAbs: ontogeny and modulation in vivo by immunosuppression. *Adv Exp Med Biol.* 1988;237:269-275.
- Klug DB, Carter C, Crouch E, Roop D, Conti CJ, Richie ER. Interdependence of cortical thymic epithelial cell differentiation and T-lineage commitment. *Proc Natl Acad Sci U S A.* 1998;95:11822-11827.
- Surh CD, Ernst B, Sprent J. Growth of epithelial cells in the thymic medulla is under the control of mature T cells. *J Exp Med.* 1992;176:611-616.
- Lind EF, Prockop SE, Porritt HE, Petrie HT. Mapping precursor movement through the postnatal thymus reveals specific microenvironments supporting defined stages of early lymphoid development. *J Exp Med.* 2001;194:127-134.

9. Anderson G, Anderson KL, Tchilian EZ, Owen JJ, Jenkinson EJ. Fibroblast dependency during early thymocyte development maps to the CD25+ CD44+ stage and involves interactions with fibroblast matrix molecules. *Eur J Immunol*. 1997;27:1200-1206.
10. Sprent J, Webb SR. Intrathymic and extrathymic clonal deletion of T cells. *Curr Opin Immunol*. 1995;7:196-205.
11. Sebzda E, Mariathasan S, Ohteki T, Jones R, Bachmann MF, Ohashi PS. Selection of the T cell repertoire. *Annu Rev Immunol*. 1999;17:829-874.
12. Farr AG, Anderson SK. Epithelial heterogeneity in the murine thymus: fucose-specific lectins bind medullary epithelial cells. *J Immunol*. 1985;134:2971-2777.
13. Degermann S, Surh CD, Glimcher LH, Sprent J, Lo D. B7 expression on thymic medullary epithelium correlates with epithelium-mediated deletion of Vbeta5+ thymocytes. *J Immunol*. 1994;152:3254-3263.
14. Gray DH, Chidgey AP, Boyd RL. Analysis of thymic stromal cell populations using flow cytometry. *J Immunol Methods*. 2002;260:15-28.
15. Godfrey DI, Izon DJ, Tucek CL, Wilson TJ, Boyd RL. The phenotypic heterogeneity of mouse thymic stromal cells. *Immunology*. 1990;70:66-74.
16. Jenkinson WE, Jenkinson E, Anderson G. Differential requirement for mesenchyme in the proliferation and maturation of thymic epithelial progenitors. *J Exp Med*. 2003;198:325-332.
17. Rossi S, Blazar BR, Farrell CL, et al. Keratinocyte growth factor preserves normal thymopoiesis and thymic microenvironment during experimental graft-versus-host disease. *Blood*. 2002;100:682-691.
18. Bustin SA. Absolute quantification of mRNA using real-time reverse transcription polymerase chain reaction assays. *J Mol Endocrinol*. 2000;25:169-193.
19. Anderson KL, Moore NC, McLoughlin DE, Jenkinson EJ, Owen JJ. Studies on thymic epithelial cells in vitro. *Dev Comp Immunol*. 1998;22:367-377.
20. Gillard GO, Farr AG. Features of medullary thymic epithelium implicate postnatal development in maintaining epithelial heterogeneity and tissue-restricted antigen expression. *J Immunol*. 2006;176:5815-5824.
21. Gerdes J, Lemke H, Baisch H, Wacker HH, Schwab U, Stein H. Cell cycle analysis of a cell proliferation-associated human nuclear antigen defined by the monoclonal antibody Ki-67. *J Immunol*. 1984;133:1710-1715.
22. Surh CD, Gao EK, Kosaka H, et al. Two subsets of epithelial cells in the thymic medulla. *J Exp Med*. 1992;176:495-505.
23. Sutherland JS, Goldberg GL, Hammett MV, et al. Activation of thymic regeneration in mice and humans following androgen blockade. *J Immunol*. 2005;175:2741-2753.
24. Heng TS, Goldberg GL, Gray DH, Sutherland JS, Chidgey AP, Boyd RL. Effects of castration on thymocyte development in two different models of thymic involution. *J Immunol*. 2005;175:2982-2993.
25. van Ewijk W, Hollander G, Terhorst C, Wang B. Stepwise development of thymic microenvironments in vivo is regulated by thymocyte subsets. *Development*. 2000;127:1583-1591.
26. Shores EW, van Ewijk W, Singer A. Disorganization and restoration of thymic medullary epithelial cells in T cell receptor-negative scid mice: evidence that receptor-bearing lymphocytes influence maturation of the thymic microenvironment. *Eur J Immunol*. 1991;21:1657-1661.
27. Derbinski J, Kyewski B. Linking signalling pathways, thymic stroma integrity and autoimmunity. *Trends Immunol*. 2005;26:503-506.
28. Burkly L, Hession C, Ogata L, et al. Expression of RelB is required for the development of thymic medulla and dendritic cells. *Nature*. 1995;373:531-536.
29. Shinkura R, Kitada K, Matsuda F, et al. Alymphoplasia is caused by a point mutation in the mouse gene encoding Nf-kappa b-inducing kinase. *Nat Genet*. 1999;22:74-77.
30. Dunn RJ, Lueddecker CJ, Haugen HS, Clegg CH, Farr AG. Thymic overexpression of CD40 ligand disrupts normal thymic epithelial organization. *J Histochem Cytochem*. 1997;45:129-141.
31. Kyewski BA, Fathman CG, Kaplan HS. Intrathymic presentation of circulating non-major histocompatibility complex antigens. *Nature*. 1984;308:196-199.
32. Lorenz RG, Allen PM. Thymic cortical epithelial cells lack full capacity for antigen presentation. *Nature*. 1989;340:557-559.
33. Mueller SN, Heath W, McLain JD, Carbone FR, Jones CM. Characterization of two TCR transgenic mouse lines specific for herpes simplex virus. *Immunol Cell Biol*. 2002;80:156-163.
34. Anderson MS, Venanzi ES, Klein L, et al. Projection of an immunological self shadow within the thymus by the aire protein. *Science*. 2002;298:1395-1401.
35. Annunziato F, Romagnani P, Cosmi L, et al. Macrophage-derived chemokine and EBI-1-ligand chemokine attract human thymocytes in different stages of development and are produced by distinct subsets of medullary epithelial cells: possible implications for negative selection. *J Immunol*. 2000;165:238-246.
36. Boehm T, Scheu S, Pfeffer K, Bleul CC. Thymic medullary epithelial cell differentiation, thymocyte emigration, and the control of autoimmunity require lympho-epithelial cross talk via LTbetaR. *J Exp Med*. 2003;198:757-769.
37. Slack JM. Stem cells in epithelial tissues. *Science*. 2000;287:1431-1433.
38. Yang SJ, Ahn S, Park CS, et al. The quantitative assessment of MHC II on thymic epithelium: implications in cortical thymocyte development. *Int Immunol*. 2006;18:729-739.
39. Robles AI, Larcher F, Whalin RB, et al. Expression of cyclin D1 in epithelial tissues of transgenic mice results in epidermal hyperproliferation and severe thymic hyperplasia. *Proc Natl Acad Sci U S A*. 1996;93:7634-7638.
40. Nasreen M, Ueno T, Saito F, Takahama Y. In vivo treatment of class II MHC-deficient mice with anti-TCR antibody restores the generation of circulating CD4 T cells and optimal architecture of thymic medulla. *J Immunol*. 2003;171:3394-3400.
41. Fontenot JD, Dooley JL, Farr AG, Rudensky AY. Developmental regulation of Foxp3 expression during ontogeny. *J Exp Med*. 2005;202:901-906.
42. Kyewski BA, Kaplan HS. Lymphoepithelial interactions in the mouse thymus: phenotypic and kinetic studies on thymic nurse cells. *J Immunol*. 1982;128:2287-2294.
43. van Ewijk W. Cell surface topography of thymic microenvironments. *Lab Invest*. 1988;59:579-590.
44. Gallegos AM, Bevan MJ. Central tolerance: good but imperfect. *Immunol Rev*. 2006;209:290-296.
45. Mizuuchi T, Kasai M, Kokuho T, Kakiuchi T, Hirokawa K. Medullary but not cortical thymic epithelial cells present soluble antigens to helper T cells. *J Exp Med*. 1992;175:1601-1605.
46. Derbinski J, Gabler J, Brors B, et al. Promiscuous gene expression in thymic epithelial cells is regulated at multiple levels. *J Exp Med*. 2005;202:33-45.
47. Gallegos AM, Bevan MJ. Central tolerance to tissue-specific antigens mediated by direct and indirect antigen presentation. *J Exp Med*. 2004;200:1039-1049.
48. Hoffmann MW, Allison J, Miller JF. Tolerance induction by thymic medullary epithelium. *Proc Natl Acad Sci U S A*. 1992;89:2526-2530.
49. Williams JA, Sharrow SO, Adams AJ, Hodes RJ. CD40 ligand functions non-cell autonomously to promote deletion of self-reactive thymocytes. *J Immunol*. 2002;168:2759-2765.
50. Punt JA, Osborne BA, Takahama Y, Sharrow SO, Singer A. Negative selection of CD4+CD8+ thymocytes by T cell receptor-induced apoptosis requires a costimulatory signal that can be provided by CD28. *J Exp Med*. 1994;179:709-713.
51. Gao JX, Zhang H, Bai XF, et al. Perinatal blockade of b7-1 and b7-2 inhibits clonal deletion of highly pathogenic autoreactive T cells. *J Exp Med*. 2002;195:959-971.
52. Tai X, Cowan M, Feigenbaum L, Singer A. CD28 costimulation of developing thymocytes induces Foxp3 expression and regulatory T cell differentiation independently of interleukin 2. *Nat Immunol*. 2005;6:152-162.



**blood**<sup>®</sup>

2006 108: 3777-3785  
doi:10.1182/blood-2006-02-004531 originally published  
online August 8, 2006

## **Developmental kinetics, turnover, and stimulatory capacity of thymic epithelial cells**

Daniel H. D. Gray, Natalie Seach, Tomoo Ueno, Morag K. Milton, Adrian Liston, Andrew M. Lew, Christopher C. Goodnow and Richard L. Boyd

---

Updated information and services can be found at:  
<http://www.bloodjournal.org/content/108/12/3777.full.html>

Articles on similar topics can be found in the following Blood collections  
[Immunobiology and Immunotherapy](#) (5662 articles)

---

Information about reproducing this article in parts or in its entirety may be found online at:  
[http://www.bloodjournal.org/site/misc/rights.xhtml#repub\\_requests](http://www.bloodjournal.org/site/misc/rights.xhtml#repub_requests)

Information about ordering reprints may be found online at:  
<http://www.bloodjournal.org/site/misc/rights.xhtml#reprints>

Information about subscriptions and ASH membership may be found online at:  
<http://www.bloodjournal.org/site/subscriptions/index.xhtml>